DOI: 10.1016/S1872-5813(21)60166-4

# Nickel oxide modified C<sub>3</sub>N<sub>5</sub> photocatalyst for enhanced hydrogen evolution performance

LIU Mu-yao<sup>1</sup>, WANG Jian-yun<sup>1</sup>, DUAN Lian<sup>1,\*</sup>, LIU Xian<sup>2,\*</sup>, ZHANG Lei<sup>3</sup>

 $(1.\,School\,of\,Chemistry\,and\,Chemical\,Engineering,\,Taiyuan\,University\,of\,Technology,\,Taiyuan\,030024,\,China;\\$ 

- 2. Department of Chemistry, Taiyuan Normal University, Jinzhong 030619, China;
- 3. Shenzhen Huace International Certification Co., Ltd, Shenzhen 518101, China)

**Abstract:** Recently, a new carbon nitride  $(C_3N_5)$  photocatalyst has attracted much attention due to its excellent light harvesting and unique 2D structure. However, high recombination rates of electron-hole pairs of bulk  $C_3N_5$  serious affect the photocatalytic performance. Herein, nickel oxide (NiO) modified  $C_3N_5$  p-n junctions photocatalyst was synthesized by a facile hydrothermal method. Results indicated that the 9-Ni/ $C_3N_5$  nanosheet photocatalyst showed excellent hydrogen production efficiency under visible light. The hydrogen production rate reached 357  $\mu$ mol/(g·h), which was 107-fold higher than that of pristine  $C_3N_5$ . The high catalytic performace was attributed to the 9-Ni/ $C_3N_5$  p-n junctions which could efficiently promote photogenerated electron-hole pair separation and thus promote the hydrogen evolution reaction.

**Key words:** hydrogen evolution; C<sub>3</sub>N<sub>5</sub> nanosheet; nickel oxide; photocatalysis

Graphitic carbon nitride  $(g-C_3N_4)$ , the most popular metal-free semiconductor, has been widely used for sunlight-driven water splitting<sup>[1-3]</sup>, carbon dioxide photoreduction<sup>[4,5]</sup> and organic pollutant photodegradation<sup>[6,7]</sup>. However, the somewhat wide bandgap of  $g-C_3N_4$  means that it can absorb only the ultraviolet and blue fraction of the solar spectrum ( $\lambda < 450$  nm), which has seriously limited its photocatalytic performance<sup>[8,9]</sup>. It has been found that the bandgap can be reduced significantly by increasing the N/C ratio<sup>[10]</sup>. Thereby, it is quite necessary to develop N-rich carbon nitride materials.

g-C<sub>3</sub>N<sub>5</sub>, as a new carbon nitride photocatalyst with high nitrogen content and narrower bandgap, showed extraordinary field properties the photocatalysis<sup>[11]</sup>. The C<sub>3</sub>N<sub>5</sub> framework contains heptazine moieties bridged together by azo linkage (-N=N-). The presence of azo linkage extends the  $\pi$ conjugated network due to overlap between the p orbitals on N atoms constituting the azo bond and  $\pi$ system of heptazine motif, which resulted in the reduction of the electronic bandgap<sup>[12]</sup>. Like most of semiconductors, g-C<sub>3</sub>N<sub>5</sub> also suffers the innate drawback of carrier recombination and low specific surface area of bulk g-C<sub>3</sub>N<sub>5</sub><sup>[13]</sup>. In the previous reports, various hybrid composites have been developed to improve the catalytic activity of  $C_3N_5$ . For example, the  $CeTi_2O_6/g$ - $C_3N_5$  heterojunction exhibited outstanding photocatalytic response under the visible light towards the degradation of endocrine rupture material 2,4-dichlorophenol (2,4-DCP) than its single component [14]. Nitrogen vacancies g- $C_3N_5/BiOBr$  composites also exhibited excellent PEC NRR performance without the addition of noble metals [15].

Nickel (II) oxide (NiO), as a non-noble metal p-type semiconductor monoxide, plays an important role in the photocatalytic hydrogen production process due to it can offer more active sites for hydrogen-releasing [16-21]. Moreover, NiO can promote the separation of photogenerated electron-hole pairs by formation of p-n junctions with other n-type semiconductors. Recently, NiO modified g- $C_3N_4$  non-noble metal heterojunction photocatalyst exhibited enhanced phototcatalytic performance for hydrogen production [22-24]. Therefore, it is possible to design NiO/ $C_3N_5$  p-n junctions photocatalysts with desirable performance. To the best of our knowledge, there is no report available for NiO/g- $C_3N_5$  composite towards the photocatalytic hydrogen evolution.

In the present work, we aimed to construct a NiO modified  $C_3N_5$  non-noble metal photocatalyst with enhanced hydrogen evolution performance. Varying

Received: 2021-06-09; Revised: 2021-08-12

The project was supported by the Teaching Reform and Innovation Program of Higher Education Institutions in Shanxi (2020061) and the Teaching Reform and Innovation Program of Taiyuan University of Technology (2019013).

<sup>\*</sup> Corresponding author. Tel: 13111006822; 18435162096, E-mail: duanlian@tyut.edu.cn, liuxian1104@126.com.

amounts of Ni modified  $C_3N_5$  samples were prepared and characterized. Based on the experimental results, it can be found that the migration and separation of photogenerated electron-hole pairs by formation of p-n junctions is beneficial to the photocatalytic hydrogen evolution performance. Furthermore, the possible photocatalytic hydrogen evolution mechanism was discussed.

## 1 Experimental

### 1.1 Preparation of bulk C<sub>3</sub>N<sub>5</sub>

All the reagents in this work were of analytical grade and used as received without any purification. Bulk C<sub>3</sub>N<sub>5</sub> had been prepared expediently from the thermal polymerization method<sup>[25]</sup>. In brief, 8 g 3-amino-1,2,4-triazole (3-AT) and 8 g NH<sub>4</sub>Cl was grounded to form a homogeneous solid mixture. The mixture was heated at 550 °C for 3 h with a ramping rate of 15 °C/min, and cooled naturally to room temperature. Finally, the obtained chocolate brown color product was dried at 70 °C in a vacuum oven for 5 h.

### 1.2 Preparation of C<sub>3</sub>N<sub>5</sub> nanosheets

The  $C_3N_5$  nanosheets were obtained according to the literature with a few modifications<sup>[26]</sup>. Simply, 1.0 g bulk  $C_3N_5$  was added into round-bottom flask containing 20 mL 3.0 mol/L nitric acid solution. The solution was stirred continuously for 24 h till it turned yellow. Then product was diluted with 1.0 L deionized water, collected by suction filtration with membrane and dried at 70 °C for 4 h. The obtained powder was named as  $C_3N_5$  nanosheets.

## 1.3 Preparation of 9-Ni/C<sub>3</sub>N<sub>5</sub> composite

The 9-Ni/C<sub>3</sub>N<sub>5</sub> sample was prepared by a hydrothermal method. Firstly, 50 mg C<sub>3</sub>N<sub>5</sub> nanosheets powder was dispersed in 80 mL of distilled water with vigorous ultrasound for 1.0 h. Thereafter, a desired amount of NiCl<sub>2</sub>·6H<sub>2</sub>O was added with continuous stirring, and then adjust the pH value 12.0 using 28% ammonia. After 0.5 h, the suspension was transferred to a 100 mL Teflon-lined stainless-steel autoclave and maintained at 150 °C for 12 h. Subsequently, the powder product was centrifugated, washed and dried at 70 °C in the vacuum drying oven. The final product was obtained after heat treatment at 300 °C for 4 h in air. The samples were named as *x*-Ni/C<sub>3</sub>N<sub>5</sub>, where *x* is the weight ratio of NiCl<sub>2</sub>·6H<sub>2</sub>O (0, 3%, 5%, 9% and 18%) to the composite.

#### 1.4 Photocatalytic H<sub>2</sub> generation

Photocatalytic  $H_2$  generation experiments were measured in a lab solar  $H_2$ -evolution system. Xe lamp with an AM 1.5 G filter (CEL-HXF300, 300 W,  $\lambda \geq$  420 nm) was used as a simulated solar light and the light density was 160 mW/cm². In a typical measurement, 50 mg NiO/C<sub>3</sub>N<sub>5</sub> composite was dispersed by ultrasound into a 100 mL triethanolamine (TEOA) solution (15%) and the system was kept at -0.1 MPa and 5 °C. GC-7900 gas chromatograph was employed to detect the  $H_2$  on line after every 1 h.

#### 2 Results and discussion

## 2.1 Characterizations of NiO/C<sub>3</sub>N<sub>5</sub> composite

The structure and morphology were observed by scanning electron microscopy (SEM) and transmission electron microscopy (TEM), as shown in Figure 1.

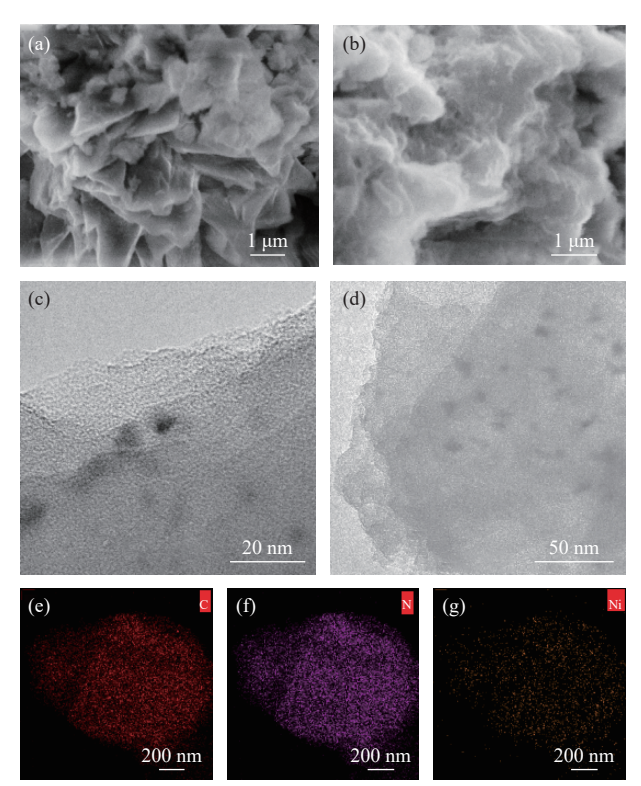


Figure 1 (a) SEM image of  $C_3N_5$  nanosheets; (b) SEM image of 9-Ni/ $C_3N_5$ ; (c) and (d) TEM images of 9-Ni/ $C_3N_5$ , (e) – (g) the corresponding elemental mapping of C, N and Ni (scale bar: 200 nm)

From Figure 1(a), it can be seen that  $C_3N_5$  shows an obvious sheet-like structure by acidifying. After modified with NiO, the dense multilayer structure was formed (Figure 1(b)), this structure was also verified by high magnification TEM image (Figure 1(c)). From Figure 1(d), we can observe that some dark nanoparticles dispersed uniformly on the multilayer of

9-Ni/C<sub>3</sub>N<sub>5</sub> and the average diameter of the black spots is about 5–6 nm, which demonstrate that NiO particles were successfully decorated on the surface of  $C_3N_5$ . The elemental mapping on the selected area shown in Figure 1(e)–(f) demonstrates a uniformly distribution of C, N and Ni atoms on the surface of the NiO/C<sub>3</sub>N<sub>5</sub> composite.

XRD patterns of the as-prepared samples are presented in Figure 2(a). All samples show strong diffraction peak at 28.1°, which is assigned to the interlayer stacking of graphitic-like structure, indicating that the lattice structure of  $C_3N_5$  remains unchanged after NiO modification, which is beneficial for photocatalytic properties of NiO/ $C_3N_5$ . Moreover, all of the NiO/ $C_3N_5$  samples exhibit a little blue-shift to about 27.1°–27.6°, suggesting that parts of Ni may implant into the lattice of  $C_3N_5$ . No obvious peak was detected after loading NiO species onto pure  $C_3N_5$ , probably because of low crystallinity and amorphous structure.

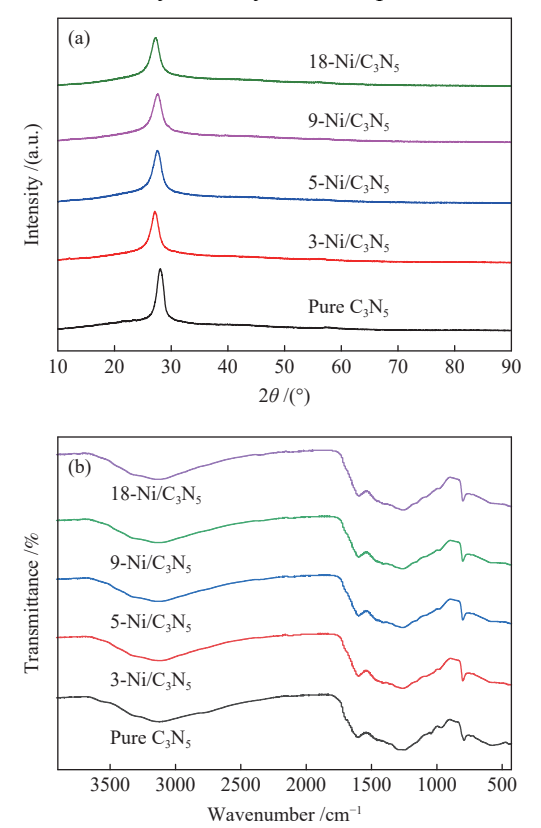


Figure 2 XRD patterns (a) and FT-IR spectra (b) for  $C_3N_5$  and x-Ni/ $C_3N_5$  composites

To gain an insight into the surface functional group of as prepared samples, the FT-IR analysis was carried out. As exhibited in Figure 2(b), there is an obvious peak at about 808 cm<sup>-1</sup>, which can be assigned to the bending vibration of triazine units<sup>[27]</sup>. In addition, the band ranged from 1200 to 1600 cm<sup>-1</sup> belongs to the

stretching in aromatic C–N. The broad peak at  $3000-3600 \text{ cm}^{-1}$  is attributed to the stretching vibration of N–H or O–H groups. The bare  $C_3N_5$  and  $Ni/C_3N_5$  nanocomposites show similar absorption bands, indicating that the structure of  $C_3N_5$  remains unchanged after NiO modification.

To analysis the composition and chemical state of constituent elements in 9-Ni/C<sub>3</sub>N<sub>5</sub> sample, XPS measurements were conducted. Referring to Figure 3(a), the XPS survey spectra of 9-Ni/C<sub>3</sub>N<sub>5</sub> sample not only exhibits the peaks of C 1s peak and N 1s peak, but also exhibits a relatively weak O 1s and Ni 2p peak, indicating the well combination of C<sub>3</sub>N<sub>5</sub> and NiO. In the C 1s spectrum (Figure 3(b)), the binding energies at 285 and 288.25 eV can be attributed to C-C and N-C=N peaks, respectively<sup>[28]</sup>. There are three peaks for the N 1s XPS peak in Figure 3(c), which are ascribed to the amino groups (400.7 eV), N(C)<sub>3</sub> (399.7 eV) and C-N=C (398.6 eV), respectively<sup>[3]</sup>. The peak of Ni spectra (Figure 3(d)) centered at 872.7 and 855.4 eV is related to Ni  $2p_{1/2}$  and Ni  $2p_{3/2}$ , respectively<sup>[29-31]</sup>. The two relatively weak satellite peaks located at 879.9 and 862.2 eV belong to the shake-up types of Ni  $2p_{1/2}$  and Ni  $2p_{3/2}$ . This result was consistent to previous literature.

# 2.2 Photocatalytic H<sub>2</sub>-production

The photocatalytic  $H_2$ -production activity of the xnanosheets evaluated Ni/C<sub>3</sub>N<sub>5</sub> was triethanolamine as an electron donor. As shown in Figure 4(a), as a controlled experiment, negligible H<sub>2</sub> was detected without either photocatalyst or irradiation. Trace H<sub>2</sub> evolution was observed for bare C<sub>3</sub>N<sub>5</sub>, while Ni-modified C<sub>3</sub>N<sub>5</sub> nanosheets displayed better H<sub>2</sub> evolution rate than bare C<sub>3</sub>N<sub>5</sub>. After loading different Ni proportions (3%, 5%, 9% or 18%) on  $C_3N_5$ nanosheets, the photocatalytic performance NiO/C<sub>3</sub>N<sub>5</sub> has been remarkably improved, and the highest amount of H<sub>2</sub> evolution of 9-Ni/C<sub>3</sub>N<sub>5</sub> can reach 357 µmol/(g·h) in the first 4 h reaction. The excellent photocatalytic H<sub>2</sub>-production activity is probably due to the separation of photogenerated electron-hole pairs by formation of p-n junctions, which can be confirmed by PL (Figure 5(a)). The PL emission intensity of 9-Ni/C<sub>3</sub>N<sub>5</sub> was the lowest among all the samples, indicating 9-Ni/C<sub>3</sub>N<sub>5</sub> has the highest separation efficiency of electrons and holes. Moreover, the BET surface area of 9-Ni/C<sub>3</sub>N<sub>5</sub> was the largest among all the samples (the BET surface area of 9-Ni/C<sub>3</sub>N<sub>5</sub> was found to be 24.6425 m<sup>2</sup>/g, which was larger than bulk C<sub>3</sub>N<sub>5</sub>  $(20.7077 \text{ m}^2/\text{g})$ ,  $3\text{-Ni/C}_3\text{N}_5$   $(22.1024 \text{ m}^2/\text{g})$ ,  $5\text{-Ni/C}_3\text{N}_5$   $(24.4835 \text{ m}^2/\text{g})$  and  $18\text{-Ni/C}_3\text{N}_5$   $(9.3544 \text{ m}^2/\text{g})$ , which was benefit to catalytic hydrogen evolution reaction.

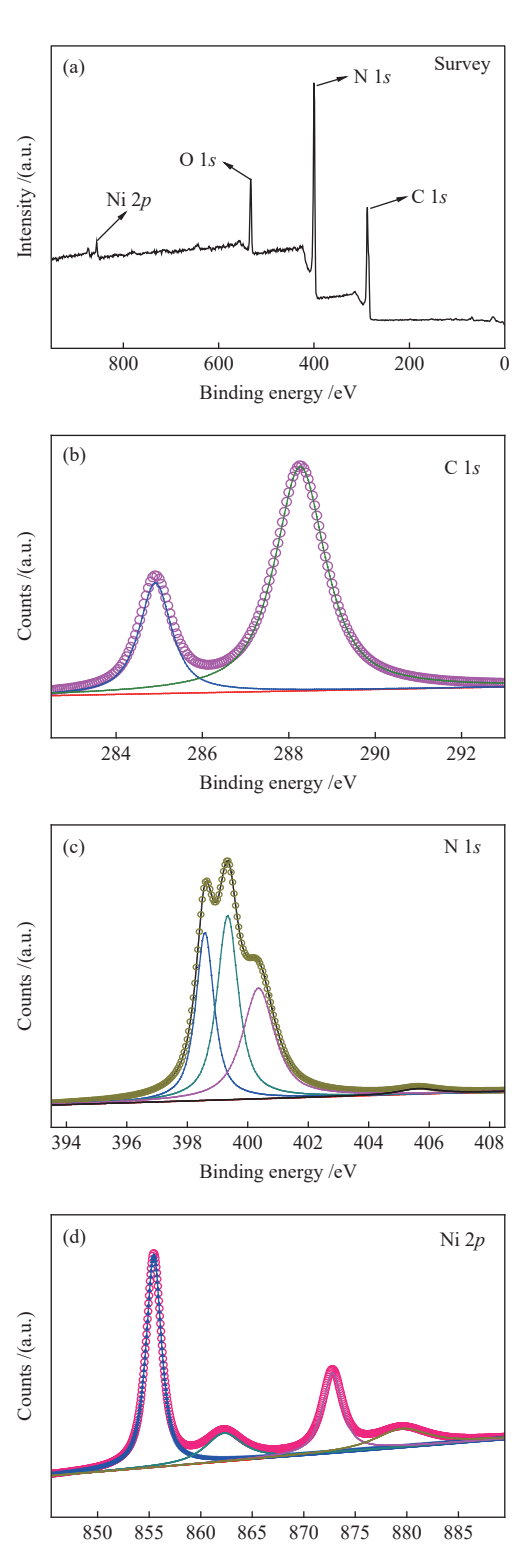


Figure 3 XPS spectra of (a) survey scan, (b) C 1s, (c) N 1s and (d) Ni 2p spectra of  $9-\text{Ni}/\text{C}_3\text{N}_5$ 

Binding energy /eV

In order to demonstrate the stability and durability of  $9-Ni/C_3N_5$ , the recycling experiments were

performed under similar experimental conditions, and each test cycle time is 4 h. As shown in Figure 4(b), the results show that the amount of H<sub>2</sub> produced was retained by about 82% after four cycles, indicating the high stability properties of 9-Ni/C<sub>3</sub>N<sub>5</sub> composite.

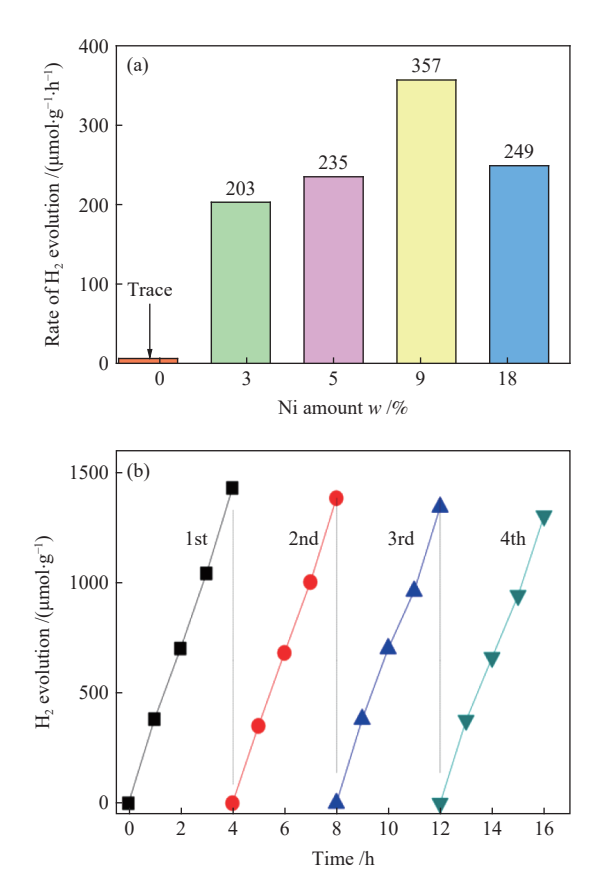


Figure 4 (a) Histogram of the photocatalytic  $H_2$  production rate of  $C_3N_5$  with varied Ni content, (b) recycle experiments of 9-Ni/ $C_3N_5$  photocatalyst

#### 2.3 Mechanism analysis

According to the results of mentioned above, the enhanced  $H_2$ -production performance of  $9\text{-Ni/C}_3N_5$  photocatalyst mainly attributes to three reasons: (1) NiO nanoparticles offer more active sites for hydrogen-releasing, (2) broaden the photo light absorption region and (3) the effective separation of photogenerated electron-hole pairs by formation of p-n junctions, which were verified further by the following experiments.

Photoluminescence (PL) spectroscopy is usually employed to investigate the optical properties and charge-separation efficiency. As shown in Figure 5(a), PL intensity of NiO/C<sub>3</sub>N<sub>5</sub> gradually increases first, and then decreases with the increase of Ni content. These results indicate that the NiO nanoparticles on  $C_3N_5$  are able to effectively promote the transfer of charge and

thus inhibit photogenerated electron-hole pairs recombination. The PL emission intensity of  $9\text{-Ni}/C_3N_5$  was the lowest among all the samples, indicating  $9\text{-Ni}/C_3N_5$  has the highest separation efficiency of electrons and holes. The time-resolved PL (TRPL) decay profiles of  $C_3N_5$  and  $9\text{-Ni}/C_3N_5$  in Figure 5(b) showed that the charge carrier lifetime in  $9\text{-Ni}/C_3N_5$  (2.386 ns) was longer than that of  $C_3N_5$  (2.006 ns). The result further indicated that  $9\text{-Ni}/C_3N_5$  has excellent separation efficiency of electrons and holes.

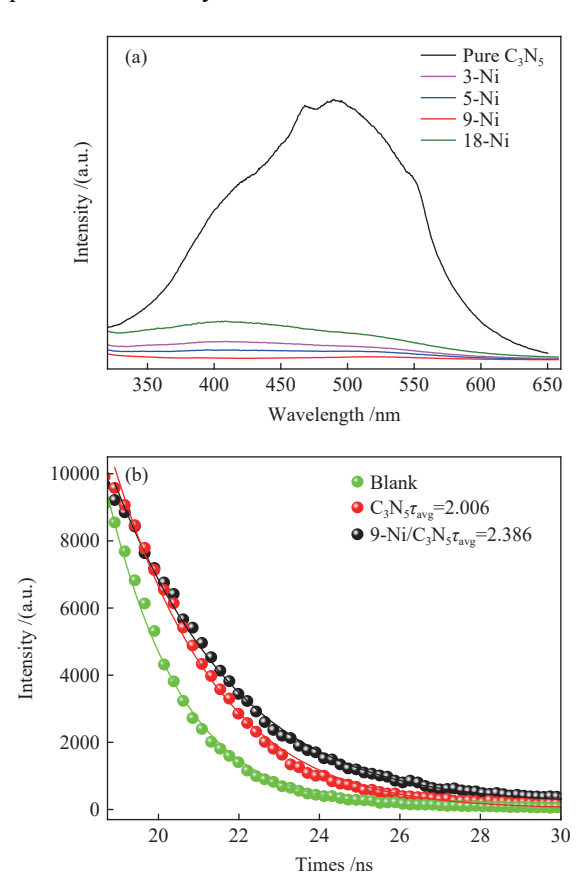


Figure 5 PL spectra (a) and TRPL spectra (b) of different samples

The optical absorption properties of the samples were tested by UV-vis absorption spectroscopy. As shown in Figure 6(a), both  $C_3N_5$  and 9-Ni/ $C_3N_5$  exhibit clear absorption in the region of visible light. Their band-gap energies are 1.95 and 1.78 eV, respectively (Figure 6(b)), which agree with previous reports well. Furthermore, 9-Ni/ $C_3N_5$  can harvest visible light more efficiently for above catalytic reaction, which may be due to a broader tail (bathochromic/red shift) in the absorption spectrum. The band positions were confirmed by Mott-Schottky plots, as depicted in Figure 6(c). The flat band or CB potential of  $C_3N_5$  was -0.67 V.

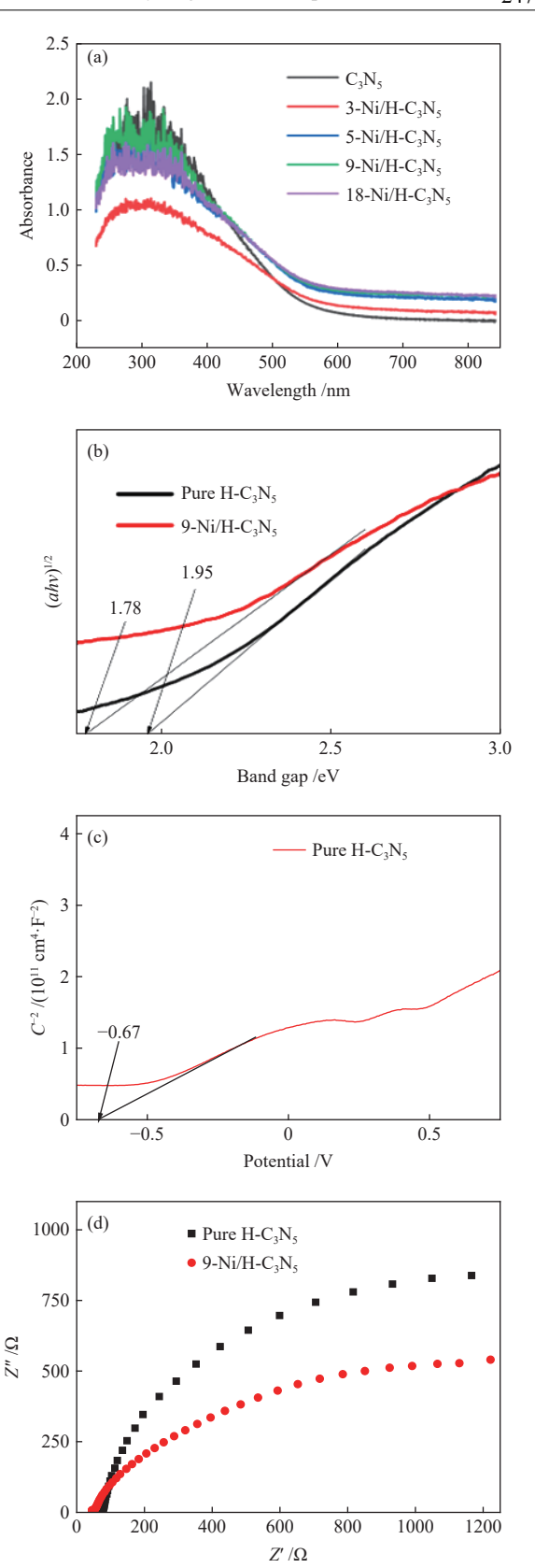


Figure 6 (a) UV-vis absorption spectra, (b) bandgap energy, (c) Mott-Schottky plots and (d) Electrochemical impedance spectra of different samples

From the obtained CB and band gap potential, it is easy to estimate the VB position of  $C_3N_5$ , which was

calculated to be 1.28 V. The positive slopes could prove the n-type semiconductors properties of  $C_3N_5$ , which was favorable to form p-n junction with p-type NiO nanoparticles. The p-n junction will promote the separation of electron-hole pairs. This result was further clarified by the electrochemical impedance spectroscopy (EIS) plot (Figure 6(d)). 9-Ni/ $C_3N_5$  has the smaller semicircle diameter compared to pure  $C_3N_5$  in higher frequency region, which indicated enhanced charge-carrier transfer ability of 9-Ni/ $C_3N_5^{[32]}$ .

Based on the results and analysis above, a possible photocatalytic H<sub>2</sub>-production mechanism over 9-Ni/C<sub>3</sub>N<sub>5</sub> photocatalyst was summarized in Figure 7.

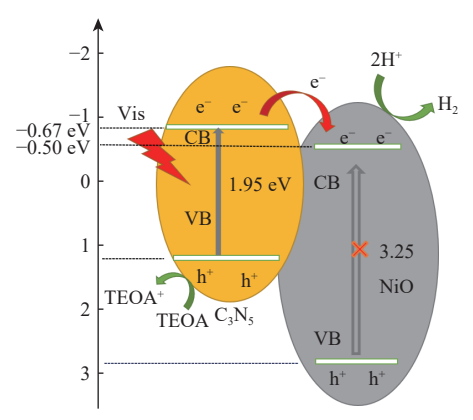


Figure 7 Proposed  $H_2$  evolution mechanism by  $9-Ni/C_3N_5$  photocatalyst

Under visible light irradiation, only  $C_3N_5$  can easily absorb visible light and generate photo-induced electron-hole pairs. Photogenerated electrons in the CB of  $C_3N_5$  migrate to the more negative potential CB of NiO ( $E_{CB} = -0.5$  V vs NHE) for proton reduction, and photogenerated holes in the VB of  $C_3N_4$  were consumed by the sacrificial electron donor TEOA. In a word, the photo-induced electron-hole pairs can be efficient separation by constructing an inner electric field of NiO/ $C_3N_5$  *p-n* heterojunction.

#### 3 Conclusions

In summary, we successfully synthesized 9-Ni/C<sub>3</sub>N<sub>5</sub> *p-n* junctions photocatalyst through a facile hydrothermal method. This photocatalyst showed excellent hydrogen production efficiency under visible light. The hydrogen production rate reached 357 μmol/(g·h), which was 107-fold higher than that of pristine C<sub>3</sub>N<sub>5</sub>. This mainly attributed to the NiO modification being able to promote photoinduced electron-hole pair separation, thus promote the hydrogen evolution reaction. This work has provided a feasible strategy to design non-noble metal modified carbon nitride for high-efficient solar conversion.

## References

- [1] LIAO G F, GONG Y, ZHANG L, GAO H Y, YANG G J, FANG B Z. Semiconductor polymeric graphitic carbon nitride photocatalysts: the "holy grail" for the photocatalytic hydrogen evolution reaction under visible light[J]. Energy Environ Sci, 2019, 12(7): 2080–2147.
- [2] HU B, CAI F P, CHEN T J, FAN M S, SONG C J, SHI W D. Hydrothermal synthesis g-C<sub>3</sub>N<sub>4</sub>/nano-InVO<sub>4</sub> nanocomposites and enhanced photocatalystic activity for hydrogen production under visible light irradiation [J]. ACS Appl Mater Interfaces, 2015, 7(33): 18247–18256.
- [3] MAO Z Y, CHEN J J, YANG Y F, WANG D J, BIE L J, FAHLMAN B D. Novel g-C<sub>3</sub>N<sub>4</sub>/CoO nanocomposites with significantly enhanced visible-light photocatalytic activity for H<sub>2</sub> evolution [J]. ACS Appl Mater Interfaces, 2017, 9(14): 12427–12435.
- [4] YE S, WANG R, WU M Z, YUAN Y P. A review on g-C<sub>3</sub>N<sub>4</sub> for photocatalytic water splitting and CO<sub>2</sub> reduction[J]. Appl Surf Sci, 2015, **358**: 15-17.
- [5] LI M L, ZHANG L X, FAN X Q, ZHOU Y J, WU M Y, SHI J L. Highly selective CO<sub>2</sub> photoreduction to CO over g-C<sub>3</sub>N<sub>4</sub>/Bi<sub>2</sub>WO<sub>6</sub> composites under visible light [J]. J Mater Chem A, 2015, **3**(9): 5189–5196.
- [6] FENG W H, ZHANG L X, FANG J Z, LU S Y, WU S X, CHEN Y, FANG Z Q. Improved photodegradation efficiency of 2, 4-DCP through a combined Q<sub>3</sub>Fe(III)-decorated porous g-C<sub>3</sub>N<sub>4</sub>/H<sub>2</sub>O<sub>2</sub> system[J]. Water Air Soil Poll, 2017, **228**(9): 373.
- [7] QIAN X F, WU Y W, KAN M, FANG M Y, YUE D T, ZENG J, ZHAO Y X. FeOOH quantum dots coupled g-C<sub>3</sub>N<sub>4</sub> for visible light driving photo-Fenton degradation of organic pollutants [J]. Appl Catal B: Environ, 2018, 237: 513–520.
- [8] CUI Y J, ZHANG G G, LIN Z Z, WANG X C. Condensed and low-defected graphitic carbon nitride with enhanced photocatalytic hydrogen evolution under visible light irradiation[J]. Appl Catal B: Environ, 2016, 181: 413–419.
- [9] DONG G H, ZHAO K, ZHANG L Z. Carbon self-doping induced high electronic conductivity and photoreactivity of g-C<sub>3</sub>N<sub>4</sub>[J]. Chem Commun, 2012, **48**: 6178–6180.
- [10] WANG H Y, LI M X, LU Q J, CEN Y M, ZHANG Y Y, YAO S Z. A mesoporous rod-like g-C<sub>3</sub>N<sub>5</sub> synthesized by salt-guided strategy: as a superior photocatalyst for degradation of organic pollutant[J]. ACS Sustainable Chem Eng, 2019, 7(1): 625–631.
- [11] QI S Y, FAN Y C, WANG J R, SONG X H, LI W F, ZHAO M W. Metal-free highly efficient photocatalysts for overall water splitting: C<sub>3</sub>N<sub>5</sub> multilayers[J]. Nanoscale, 2020, **12**(1): 306–315.
- [12] KUMAR P, VAHIDZADEH E, THAKUR U K, KAR P, ALAM K M, GOSWAMI A, MANDI N, CUI K, BERNARD G M, MICHAELIS V K, SHANKAR K. C<sub>3</sub>N<sub>5</sub>: A low band gap semiconductor containing an azo-linked carbon nitride framework for photocatalytic, photovoltaic and adsorbent applications [J]. J Am Chem Soc, 2019, 141(13): 5415–5436.

- [13] JIN Z B, WEI T T, HUANG J Y, LI F Y, YANG Y, XU L. Fabrication of direct Z-scheme heterojunction between Zn<sub>0.5</sub>Cd<sub>0.5</sub>S and N-rich graphite carbon nitride for boosted H<sub>2</sub> production [J]. Int J Hydrogen Energy, 2020, 45(43); 22711–22721.
- [14] VADIVEL S, HARIGANESH S, PAUL B, MAMBA G, PUVIARASU P. Highly active novel CeTi<sub>2</sub>O<sub>6</sub>/g-C<sub>3</sub>N<sub>5</sub> photocatalyst with extended spectral response towards removal of endocrine disruptor 2, 4-dichlorophenol in aqueous medium[J]. Colloids Surf A, 2020, **592**(5): 124583.
- [15] LI M X, LU Q J, LIU M L, YIN P, WU C Y, LI H T, ZHANG Y Y, YAO S Z. Photoinduced charge separation via the double-electron transfer mechanism in nitrogen vacancies g-C<sub>3</sub>N<sub>5</sub>/BiOBr for the photoelectrochemical nitrogen reduction[J]. ACS Appl Mater Interfaces, 2020, 12(34): 38266–38274.
- [16] SHI H L, BI J G, BAI C P, WU J B, XU Y, HAN Y, ZHANG X. Nickel ammine complex-derived NiO modified g-C<sub>3</sub>N<sub>4</sub> composites with enhanced visible-light photocatalytic H<sub>2</sub> evolution performance [J]. ChemistrySelect, 2019, 4(27): 8095–8103.
- [17] LIU J N, JIA Q H, LONG J L, WANG X X, GAO Z W, GU Q. Amorphous NiO as co-catalyst for enhanced visible-light-driven hydrogen generation over g-C<sub>3</sub>N<sub>4</sub> photocatalyst [J]. Appl Catal B: Environ, 2018, 222: 35–43.
- [18] HU C, TENG H. Structural features of p-type semiconducting NiO as a co-catalyst for photocatalytic water splitting[J]. J Catal, 2010, 272(1): 1–8
- [19] CHEN C, LIAO C, HSU K, WU Y, WU J. P-N junction mechanism on improved NiO/TiO<sub>2</sub> photocatalyst[J]. Catal Commun, 2011, **12**(14): 1307–1310.
- [20] LIN H, CHEN Y, CHEN Y. Water splitting reaction on NiO/InVO<sub>4</sub> under visible light irradiation [J]. Int J Hydrogen Energy, 2007, 32(1): 86–92.
- [21] SREETHAWONG T, SUZUKI Y, YOSHIKAWA S. Photocatalytic evolution of hydrogen over mesoporous supported NiO photocatalyst prepared by single-step sol-gel process with surfactant template [J]. Int J Hydrogen Energy, 2005, 30(10): 1053–1062.
- [22] IWASZUK A, NOLAN M, JIN Q, FUJISHIMA M, TADA H. Origin of the visible-light response of nickel(II) oxide cluster surface modified titanium(IV) dioxide [J]. J Phys Chem C, 2013, 117(6): 2709–2718.
- [23] FU Y, LIU C A, ZHU C, WANG H, DOU Y, SHI W, SHAO M, HUANG H, LIU Y, KANG Z. High-performance NiO/g-C<sub>3</sub>N<sub>4</sub> composites for visible-light-driven photocatalytic overall water splitting[J]. Inorg Chem Front, 2018, 5(7): 1646–1652.
- [24] TZVETKOV G, TSVETKOV M, SPASSOV T. Ammonia-evaporation-induced construction of three-dimensional NiO/g-C<sub>3</sub>N<sub>4</sub> composite with enhanced adsorption and visible light-driven photocatalytic performance[J]. Superlattice Microst, 2018, 119: 122–133.
- [25] LIU T, YANG G, WANG W, WANG C, WANG M, SUN X, XU P, ZHANG J. Preparation of C<sub>3</sub>N<sub>5</sub> nanosheets with enhanced performance in photocatalytic methylene blue (MB) degradation and H<sub>2</sub>-evolution from water splitting [J]. Environ Res, 2020, 188: 109741.
- [26] LUO B, SONG R, GENG J, JING D, ZHANG Y. Facile preparation with high yield of a 3D porous graphitic carbon nitride for dramatically enhanced photocatalytic H<sub>2</sub> evolution under visible light[J]. Appl Catal B: Environ, 2018, 238(15): 294–301.
- [27] LIN X, XU D, ZHENG J, SONG M, CHE G, WANG Y, YANG Y, LIU C, ZHAO L, CHANG L. Graphitic carbon nitride quantum dots loaded on leaf-like InVO<sub>4</sub>/BiVO<sub>4</sub> nano-heterostructures with enhanced visible-light photocatalytic activity [J]. J Alloys Compd, 2016, **688**(15): 891–898.
- [28] WANG X, MA Z, CHAI L, XU L, ZHU Z, HU Y, QIAN J, HUANG S. MOF derived N-doped carbon coated CoP particle/carbon nanotube composite for efficient oxygen evolution reaction [J]. Carbon, 2019, 141: 643-651.
- [29] KONG L, DONG Y, JIANG P, WANG G, ZHANG H, ZHAO N. Light-assisted rapid preparation of a Ni/g-C<sub>3</sub>N<sub>4</sub> magnetic composite for robust photocatalytic H<sub>2</sub> evolution from water[J]. J Mater Chem A, 2016, 4(25): 9998–10007.
- [30] HAN Q, WANG B, ZHAO Y, HU C, QU L. A graphitic-C<sub>3</sub>N<sub>4</sub> "seaweed" architecture for enhanced hydrogen evolution[J]. Angew Chem Int Ed, 2015, **54**(39): 11433–11437.
- [31] JIANG Z, CHEN X, LU J, LI Y, WEN T, ZHANG L. Ultrathin Ni(II)-based coordination polymer nanosheets as a co-catalyst for promoting photocatalytic H<sub>2</sub> production[J]. Chem Commun, 2019, 55(46): 6499.
- [32] WEN J, XIE J, ZHANG H, ZHANG A, LIU Y, CHEN X, LI X. Constructing multifunctional metallic Ni interface layers in the g-C<sub>3</sub>N<sub>4</sub> nanosheets/amorphous NiS heterojunctions for efficient photocatalytic H<sub>2</sub> generation [J]. ACS Appl Mater Interfaces, 2017, 9(16): 14031–14042.

# NiO 改性 C<sub>3</sub>N<sub>5</sub> 光催化剂析氢性能研究

刘慕瑶',王建云',段 炼1\*,刘 宪2\*,张 磊3

(1. 太原理工大学, 化学化工学院, 山西 太原 030024; 2. 太原师范学院, 化学系, 山西 晋中 030619;

3. 深圳华测国际认证有限公司, 广东 深圳 518101)

摘 要: 近年来, 新型光催化剂氮化碳( $C_3N_5$ )因其优异的光捕获性能和独特的二维结构备受关注。然而, 较高的电子-空穴复合率严重影响其光催化性能。本研究采用水热法成功合成了氧化镍( $N_iO$ )改性的  $C_3N_5$  p-n 异质结纳米光催化剂。结果表明,  $9-N_i/C_3N_5$  纳米光催化剂在可见光照射下表现出优异的析氢性能, 其析氢速率可高达 357  $\mu$ mol/(g·h), 是纯  $C_3N_5$  的 107 倍。这主要归因于  $9-N_i/C_3N_5$  纳米光催化剂形成 p-n 异质结, 有效促进了光生电子-空穴对的分离, 从而提高了析氢效率。 关键词: 制氢;  $C_3N_5$  纳米片;  $N_iO_5$  光催化

中图分类号: O643 文献标识码: A